2026 JULY 19–22 VANCOUVER, BC
JOINT AAPM | COMP MEETING

Dosimetric Analysis for a Modern ^{131}Cs Brachytherapy Seed

Alana Pankopf, Sc.M.[1]; Grace MacDonald, Sc.M.[1]; Chris Tien, PhD; Eric Hall, PhD[1]; Mark Rivard, PhD[1]

[1]Brown University, Brown University Health Cancer Institute

ABSTRACT

Purpose: Commercial ^{131}Cs brachytherapy seeds incorporate an internal gold marker for visualization on planar radiographs. As post-implant assessment shifts toward CT-based imaging, this high-Z marker introduces beam-hardening and streak artifact that degrade image quality. This work characterizes prototype ^{131}Cs seed designs that retain the external geometry while eliminating the gold marker, and quantifies the dosimetric impact.

Methods: MCNP6 was used to model three ^{131}Cs seed geometries: (1) the CS-1 Rev2 baseline (AAPM TG-43U1S2), (2) a marker-free design with argon gas replacing the gold rod, and (3) a solid ceramic-core design without the gold rod or borosilicate layer. Each design was simulated in vacuum and liquid water to derive TG-43 parameters, with WAFAC angular-averaging corrections applied.

Results: The dose distributions and dosimetry parameters agreed with the reference consensus data within 0.1%. The radial dose function and dose-rate constant changed <1% for the three designs. Removal of the Au marker resulted in 18% higher photon emissions and as a result, less 131Cs is needed for the same absorbed dose. Removal of the Au marker also resulted in more uniform dose distributions with the 2D anisotropy function having larger values than the baseline. This was especially pronounced along the seed long-axis with 10% changes observed at small radii (r≤1cm) and low polar angles (θ≤10°).

Conclusions: Eliminating the gold marker preserves clinically relevant TG-43 dosimetry while improving photon emission efficiency, supporting marker-free and solid-core designs as manufacturable, imaging-compatible alternatives.

CONTACT

Alana Pankopf
Brown University
Email: alana_Pankopf@alumni.brown.com
Phone: (775) 843-7621

INTRODUCTION

Permanent interstitial brachytherapy delivers highly localized dose to malignancies such as prostate cancer and intracranial tumors by implanting small sealed radioactive sources directly into or adjacent to the target. Seed dosimetry, photon energy spectrum, self-attenuation, and angular emission pattern, depends strongly on internal construction, so accurate characterization is essential for reliable treatment planning.

Cesium-131 (^{131}Cs) has seen growing clinical use since 2004 for permanent prostate implants and surgically placed platforms such as GammaTile. Its short 9.7-day half-life and ~30 keV mean photon energy enable rapid dose delivery, potentially shortening the duration of radiation exposure to surrounding tissue.

Commercial ^{131}Cs seeds consist of a Cs-bearing ceramic matrix encapsulated in titanium, built around a central gold marker originally included to enhance radiographic visibility on 2D films. Modern post-implant evaluation increasingly relies on CT and MRI, however, and gold's high atomic number and density produce beam-hardening and streak artifact on CT and can distort MRI signal, degrading seed localization.

This motivates redesigning the internal seed structure to reduce imaging artifact while preserving external geometry and structural integrity. Because internal material changes alter photon attenuation, scattering, and anisotropy, any redesign requires full TG-43 re-characterization; Monte Carlo codes such as MCNP provide an established framework for this evaluation.

This study used MCNP6 to model the CS-1 Rev2 baseline seed alongside two marker-free alternatives, quantifying the impact on source strength, dose-rate constant, radial dose function, and 2D anisotropy function.

METHODS AND MATERIALS

Three ^{131}Cs seed geometries (active length 4.0 mm) were modeled in MCNP6 (MODE P) using macrobodies with manufacturer-specified dimensions (Fig. 1): (1) **CS-1 Rev2 baseline**, gold marker surrounded by borosilicate glass and a Cs-bearing ceramic matrix; (2) **marker-free**, gold replaced by argon gas of identical volume; (3) **solid core**, gold and borosilicate replaced by continuous ceramic matrix. All designs retained identical titanium encapsulation.

Photon emission was defined via SDEF using NuDat 3.0 ^{131}Cs energies/probabilities (29–34 keV); cross-sections were from ENDF/B-VIII. Each geometry was run in vacuum (air-kerma strength) and in a 15 cm liquid-water phantom (dose rate) for 2×10^9 histories each, giving statistical uncertainties ≤0.1% (k=1).

TG-43 line-source parameters, s_K, dose-rate constant Λ, radial dose function $g_l(r)$, and 2D anisotropy F(r,θ), were derived per AAPM TG-43U1S2, with NIST-traceable WAFAC angular-averaging corrections applied to s_K and dose rate. The baseline model was validated against published Monte Carlo data (Rivard et al.) before inter-design comparison.

RESULTS

The baseline CS-1 Rev2 model reproduced published Monte Carlo dosimetry within 0.2% for Λ, ≤1.0% for $g_l(r)$, and ≤0.1% for F(r,θ), validating the Monte Carlo implementation.

Removing the internal gold marker increased s_K by 18.9% (marker-free) and 18.1% (solid core) relative to baseline (Table 1), reflecting reduced photoelectric self-attenuation.

The dose-rate constant Λ remained essentially unchanged: 1.047, 1.045, and 1.041 $cGy\cdot h^{-1}\cdot U^{-1}$ for CS-1 Rev2, marker-free, and solid-core designs, respectively (Table 2). WAFAC corrections to s_K and dose rate changed Λ by <0.1% for all three designs.

The radial dose function $g_l(r)$ overlapped closely for all three designs across 0.05–15 cm, with differences <2% at small radii and <0.5% beyond 0.5 cm (Fig. 2).

The 2D anisotropy F(r,θ) was the most sensitive parameter (Fig. 3): F(0.5 cm, 0°) fell from 0.835 (baseline) to 0.789 (marker-free) and 0.753 (solid core), converging to <2% by θ=30°.

Total combined standard uncertainties (k=1) were ≤1.8% for all dosimetric quantities evaluated, dominated by mass energy-absorption coefficient and Monte Carlo statistical terms.

Table 1. Air-kerma strength per unit activity, s_K, for the three seed models (MCNP), with ratio relative to baseline.

Seed model	s_K (MeV/g/sp)	Ratio
CS-1 Rev2	2.603E-6	—
No Au marker	3.095E-6	1.189
Solid core	3.075E-6	1.181

Table 2. Dose-rate constant, Λ ($cGy\cdot h^{-1}\cdot U^{-1}$), for the three seed models, uncorrected and WAFAC-corrected.

Correction applied	TG-43U1S2	CS-1 Rev2	Marker Free	Solid core
Uncorrected (no WAFAC)	1.046	1.047	1.045	1.041
WAFAC applied to s_K	1.046	1.047	1.045	1.041
WAFAC applied to s_K and $\dot{D}$	—	1.047	1.045	1.040

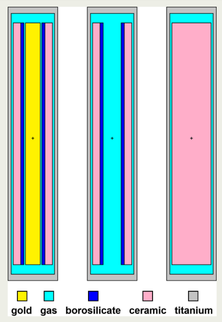

Figure 1. Cross-sections of the CS-1 Rev2 baseline (left), marker-free (middle), and solid-core (right) seed designs from the MCNP geometry.

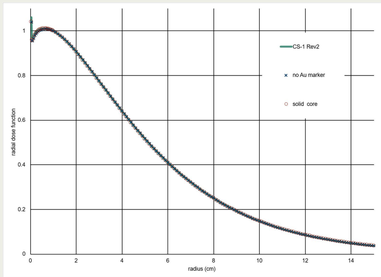

Figure 2. Radial dose function, $g_l(r)$, normalized to unity at r=1 cm, θ=90°. Results overlap closely for all three designs (0.05≤r≤15 cm).

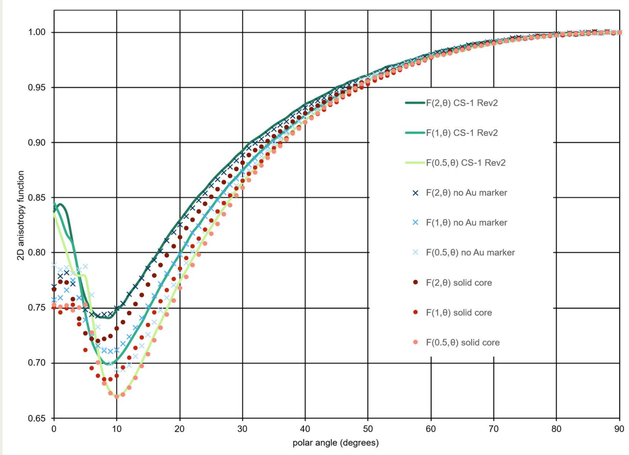

Figure 3. 2D anisotropy function, F(r,θ), for the three seed models at r = 0.5, 1.0, and 2.0 cm. Scattered photons dominate at larger distances, reducing angular sensitivity to source geometry.

DISCUSSION

Close agreement between the validated CS-1 Rev2 model and published Monte Carlo data confirms that the geometry, materials, and scoring methodology used here reliably reproduce TG-43 reference dosimetry, providing a trustworthy baseline for evaluating the redesigned seeds.

The ~18–19% increase in air-kerma strength is attributed almost entirely to eliminating photoelectric absorption in the high-Z gold rod, which previously attenuated a substantial fraction of ^{131}Cs emissions before escape. The slightly lower s_K of the solid-core design shows that internal geometry, not simply total ^{131}Cs loading, governs photon yield, permitting reduced per-seed activity for a given clinical strength.

The near-invariance of Λ is expected: both the reference dose rate and s_K scale with total photon emission, so escape-probability changes affect numerator and denominator similarly. Marker-free designs could therefore be adopted without substantial recalibration of dose-rate constants.

The radial dose function's $g_l(r)$ stability confirms that dose falloff in water is governed by scatter and attenuation in the medium rather than internal seed structure, since the emission spectrum and external geometry are unchanged.

The 2D anisotropy function was the most structurally sensitive parameter, reflecting angular photon-escape probability before water scatter dominates. Removing the gold marker produced smoother, more isotropic emission near the seed's long axis; these deviations were confined to small angles and radii and should average out across multi-seed implants.

CONCLUSIONS

Eliminating the internal gold marker from the CS-1 Rev2 ^{131}Cs seed increases air-kerma strength by ~18–19% by removing high-Z photoelectric attenuation, while preserving clinically relevant TG-43 dosimetry: the dose-rate constant changed by <0.7%, WAFAC corrections altered Λ by <0.1%, and the radial dose function agreed with baseline to within 1% beyond 0.5 cm.

The 2D anisotropy function showed localized differences near the seed's long axis, where marker-free designs produced more uniform, isotropic emission; these differences diminished rapidly with increasing angle and radius.

Overall, the marker-free and solid-core seed designs are dosimetrically comparable to the conventional CS-1 Rev2 model and represent manufacturable alternatives that may improve compatibility with CT- and MRI-based post-implant imaging workflows without compromising treatment planning accuracy or clinical performance.

REFERENCES

1. Rivard MJ, et al. Update of AAPM Task Group No. 43 Report. Med Phys. 2004;31:633–674.
2. Werner CJ, et al. MCNP User's Manual, Code Version 6.2. LA-UR-17-29981, Los Alamos National Laboratory, 2017.
3. Rivard MJ. Brachytherapy dosimetry parameters calculated for a ^{131}Cs source. Med Phys. 2007;34:754–762.
4. DeWerd LA, et al. AAPM TG-138/GEC-ESTRO dosimetric uncertainty analysis for brachytherapy sources. Med Phys. 2011;38:782–801.
5. Wang J, Zhang H. Dosimetric characterization of CS-1 Rev2 ^{131}Cs source with MCNP5. Med Phys. 2008;35:1571–1579.

© Poster Template by Genigraphics® 1.800.790.4001 www.genigraphics.com